ELSEVIER

Physica C 315 (1999) 145–153

PHYSICA C

Determination of the current density distribution in Josephson junctions

M. Carmody [a,b,*], E. Landree [b], L.D. Marks [b], K.L. Merkle [a]

[a] *Materials Science Division and Science and Technology Center for Superconductivity, Argonne National Laboratory, Argonne, IL 60439, USA*

[b] *Materials Science and Engineering Department, Northwestern University, Evanston, IL 60208, USA*

Received 4 November 1998; accepted 10 February 1999

Abstract

A technique is described for recovering the missing phase information for a set of critical current measurements as a function of an applied magnetic field $I_c(B)$. In many cases the current density $j(x)$ across the boundary for a Josephson junction can be determined.

PACS: 74.25.Fy; 74.25.Ha; 73.40.Gk

Keywords: Josephson junctions; Phase retrieval; Critical current density

1. Introduction

Most high angle grain boundaries in high-T_c superconductors exhibit the Josephson effect that can be exploited for potential device applications. Variations in grain boundary structure caused by microfaceting, macroscopic grain boundary meandering, and grain boundary precipitates cause variations in the tunneling current across the boundary. To date, there is little research that correlates the structure of the boundary to the transport properties across it.

Fig. 1 shows a schematic of the basic Josephson junction geometry that will be used for discussion. The basic equation relating the modulation of the critical current as a function of applied magnetic field across a Josephson junction can be written as a Fourier transform [1,2] such that

$$I_c(\beta) = \left| \int_{-\infty}^{\infty} j(x) \exp(i\beta x) \mathrm{d}x \right|, \qquad (1)$$

where $j(x)$ is the current density flowing in the z-direction along the length of the boundary (see Fig. 1), $\beta = 2\pi D\mu_o H_y/\Phi_o$ is the normalized magnetic field where H_y is the magnetic field threading the junction including both the applied magnetic field and the field generated by the currents flowing in the junction, and μ_o is the permeability of free space. Φ_o is defined as the superconducting flux quantum ($h/2e = 2.07 \times 10^{-7}$ G cm^2) and $D = \lambda_1 + \lambda_2 + d$ where d is the thickness of the barrier and λ the London penetration depth of the superconductors on

* Corresponding author. Argonne National Laboratory, Materials Science Division and Science and Technology Center for Superconductivity, Bldg. 212, Argonne, IL 60439, USA. Tel.: +1-630-252-5181; E-mail: carmody@an1.gov

0921-4534/99/$ - see front matter
PII: S0921-4534(99)00189-6

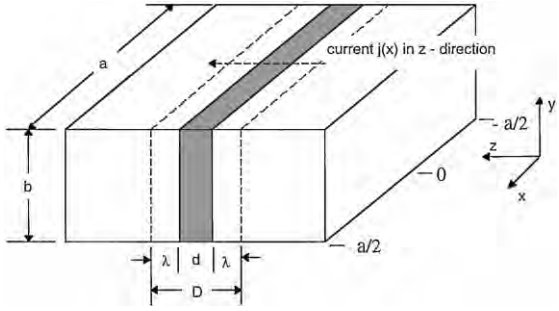

Fig. 1. Schematic of Josephson junction used for illustration of junction terms.

each side of the barrier. For a grain boundary junction, it is usually assumed that the London penetration depth (λ) is the same on both sides of the junction $(\lambda_1 = \lambda_2)$ and that the width of the grain boundary (d) is negligibly small compared to 2λ such that $D \approx 2\lambda$.

Experimentally, $I_c(B)$, where $B = \mu_o H$, is measured to analyze the junction current response for an applied magnetic field. If the current distribution is uniform, Eq. (1) simplifies to the familiar Fraunhofer diffraction pattern:

$$I_c(\beta) = I_{max}|\sin(\beta a/2)/(\beta a/2)| \qquad (2)$$

where a is the junction width as illustrated in Fig. 1. However, for most real junctions, the current distribution along the boundary is not uniform.

Since $I_c(\beta)$ from Eq. (1) is defined as the modulus of the Fourier transform of $j(x)$, the real space positional current density profile is not measured. However, if it is possible to restore the missing phase information, then calculation of the positional current density $j(x)$ along the boundary would be possible.

To reconstruct $j(x)$ from $I_c(\beta)$, both the modulus and the phase are required. Since the modulus is measured experimentally, the problem becomes one of restoring the phase $\phi(\beta)$.

Dynes and Fulton [2] attempted to solve for $j(x)$ by assuming a minimum-phase-type function. By making this assumption it was possible to use the formalisms of Hilbert transforms [3] to calculate $j(x)$ directly. Zappe [4] showed that the minimum-phase assumption used by Dynes and Fulton is not in general a valid assumption for a Josephson junction. Zappe argued that without making further assumptions about $j(x)$, it was impossible to reconstruct $j(x)$ from $I_c(\beta)$ uniquely because there can be multiple one-dimensional (1-D) real space objects $j(x)$ that when Fourier transformed produce the same modulus $I_c(\beta)$.

The problem of phase retrieval is not a new subject [5–7]. In general, without further information about the phase or the real space object it is not possible to uniquely determine the phase from moduli measurements. However, in most cases, other information or 'constraints' exist that can be used to solve the phase problem. Many iterative algorithms for phase recovery have been developed. One of the first was developed by Gerchberg and Saxton [5] and Gerchberg [6] which utilizes a series of iterative Fourier transforms to find the missing phases, otherwise known as the Gerchberg–Saxton error-reduction algorithm. The method was further improved with the use of a feedback approach and evolved into what is known as the input–output algorithm [7,8]. The phase restoration algorithm described hereafter is a modified version of the input–output algorithm developed by Gerchberg and Saxton.

The general approach involves iterative Fourier transformation back and forth between the object domain and the Fourier domain. Fig. 2 is a schematic of the generalized Gerchberg–Saxton algorithm.

This generalized algorithm for phase retrieval using iterative Fourier transforms is best explained in

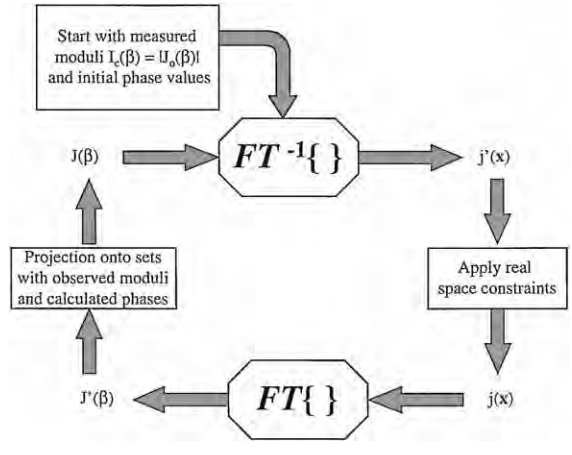

Fig. 2. Flow chart of Gerchberg–Saxton type phase retrieval algorithm used for solving current density profiles $j(x)$.

terms of set-theoretic methods involving successive projection onto sets [9], an iterative method that finds feasible solutions consistent with a set of constraints which are defined by a priori information about the real space object [9]. A feasible solution is defined as any solution that satisfies the constraints [9]. It is found by successively projecting an initial estimate of the object onto the constraint sets. This method involving mathematical projection operators can be generalized to involve non-convex constraint sets and is known as the method of generalized projections (MGP).

The algorithm used to solve the phase restoration problem for Josephson junctions involves projecting an initial estimate onto two constraint sets. The first constraint set (S_1) corresponds to the set of all solutions whose value is confined by the known object constraints. The second set (S_2) is the set of all solutions whose moduli are equal to those of the experimentally measured moduli and may be written as:

$$S_1 = \{ j(x) : j(x) = 0, \quad |x| > a/2 : J_c \geq j(x) \geq 0 : j(x) = \text{real} \}, \tag{3}$$

$$S_2 = \{ j(x) : |\mathrm{FT}\{ j(x) \}| = I_c(\beta) \}. \tag{4}$$

It can be shown that the constraint set S_1 is a closed convex set and the set S_2 is a non-convex set [9,10].

The phase retrieval algorithm can be written in terms of mathematical projections as;

$$j_{n+1} = T_2 T_1 j_n = T j_n, \tag{5}$$

where j_{n+1} is the current best estimate of j, j_n is the previous estimate of j and T_1 and T_2 are projection operators (defined by Eqs. (3) and (4)), represented by T, such that when T operates on j_n it produces j_{n+1}. T_1 corresponds to the correction of the function, j_n, with the experimentally observed moduli, $J_o(\beta)$, and T_2 is the correction for the real space constraints:

$$T_1 = 1 + \delta_1 (P_1 - 1), \tag{6}$$

$$T_2 = 1 + \delta_2 (P_2 - 1) \tag{7}$$

where

$$P_1 J(\beta) = J_o(\beta) \tag{8}$$

and $J(\beta)$ is obtained from the mapping of $j(x)$ into $J(\beta)$ via a Fourier transformation. P_2 is defined such that

$$P_2 j(x) = \begin{cases} j(x): & 0 \leq j(x) \leq J_c(x) \\ (1 - \delta_2) j(x): & j(x) < 0 \\ J_c - (\delta_2 - 1): & j(x) > J_c \\ (1 - \delta_2) j(x): & |x| > a/2 \end{cases} \tag{9}$$

where δ_1 and δ_2 are scalar constants between 1 and 2 and J_c is the bulk critical current density across the junction. When $\delta_1 = \delta_2 = 1$, the phase retrieval algorithm is identical to the Gerchberg–Saxton algorithm [10].

If one or more of the constraint sets is non-convex then it is possible that the convergence may take place locally. Specifically, there can exist various local minima all consistent with the object constraints [11]. Since multiple solutions are possible when projecting onto non-convex sets it is important to rigorously search solution space to find all possible solutions.

2. Phase retrieval algorithm

The measured moduli $I_c(\beta)$ are initially seeded with phases. The initial phases and measured moduli are then inverse Fourier transformed into real space where the real space domain constraints are applied by a projection onto sets operation [8]. The solution is then Fourier transformed back to reciprocal space where the new moduli are corrected using a projection onto sets [10] operation of the form of Eq. (8).

For the 1-D phase restoration problem a genetic algorithm [12–14] has been applied to search for the best starting set of phases (typically the strongest 10%) such that after a fixed number of iterations the solution converges to the best possible fit of the applied constraints. The initial phase guesses need only be approximate values, therefore quadrant searching $(\pi/4,\ 3\pi/4,\ 5\pi/4,\ 7\pi/4)$ or binary searching $(0 \text{ or } \pi)$ is sufficient.

After each iteration of the algorithm, a figure of merit (FOM) was calculated to monitor the convergence of each solution and was later used by the genetic algorithm to rank the solutions. Each population of the genetic algorithm is run for a relatively

small number of iterations to avoid overconvergence of the solutions. After a final solution set was obtained, the solutions were re-run for a larger number of iterations to push the solutions to a lower FOM.

It is important at this point to make a distinction between two possible situations. The missing phase information contains all information pertaining to the actual structure. Therefore, in order to make no assumptions about the solution, one must consider solutions that are centrosymmetric as well as non-centrosymmetric. This is particularly important when deciding how to define the possible initial phases, either binary or quadrant searches. If one only considers the quadrant searches, one reduces the possibility of finding solutions that may be centrosymmetric in nature in favor of a non-centrosymmetric solution. It is possible for a solution to be nearly centrosymmetric or 'pseudo-centrosymmetric'. By enforcing a centrosymmetric search algorithm (phases are only allowed to be 0 or π), one finds a solution that is close to the correct solution. Using these starting phases and then allowing the solution to refine for a larger number of iterations and allowing the phases to vary between 0 and 2π, from these pseudo-centrosymmetric starting values it finds the non-centrosymmetric solution.

Therefore, for each set of measured moduli, it is necessary to run under two different conditions, a true non-centrosymmetric (quadrant search) and a pseudo-centrosymmetric algorithm (whose search strategy begins by searching for the best solution whose phases are confined to be either 0 or π). Then using the best set of solutions for both cases as starting phases for a non-centrosymmetric solution

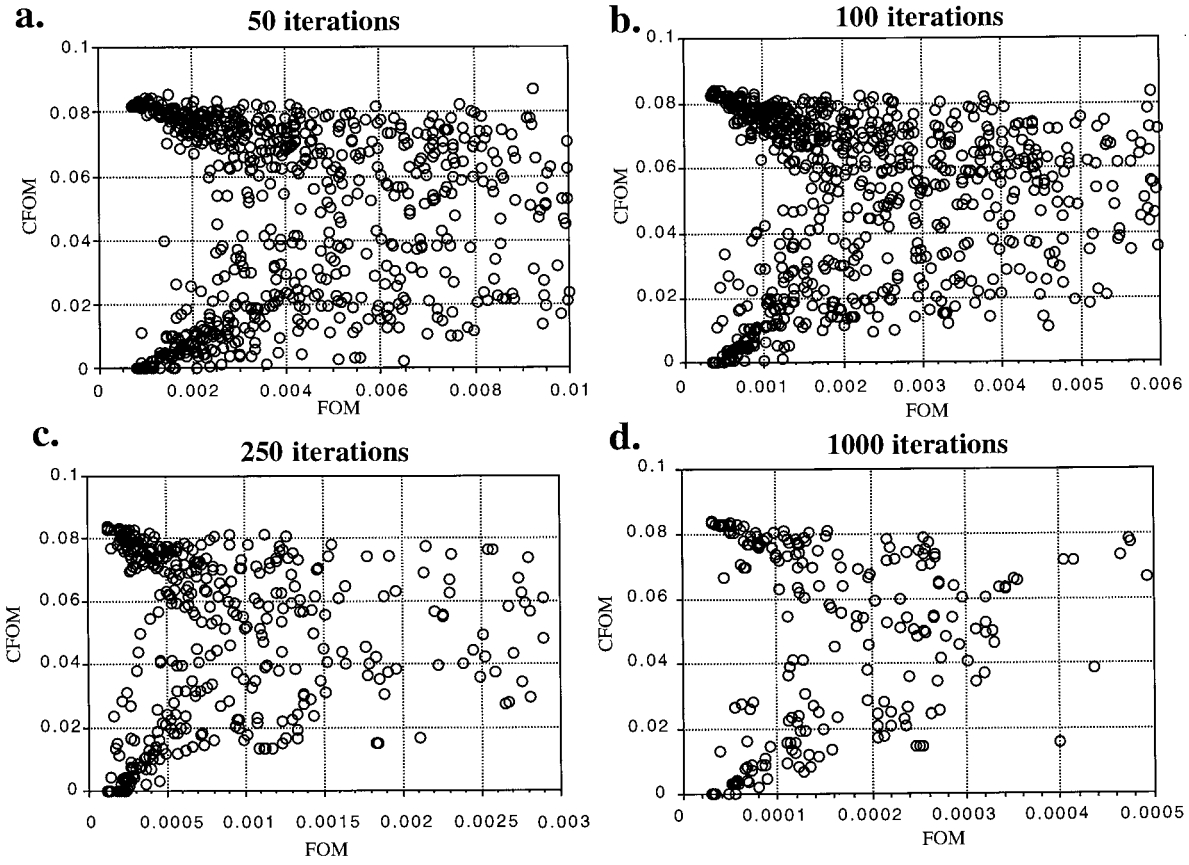

Fig. 3. Correctness factor (CFOM) vs. figure of merit (FOM) for (a) 50, (b) 100, (c) 250, and (d) 1000 iterations of the phase retrieval algorithm for the Zappe model. Two distinct solutions are evident.

refinement (allowing phases to be anything between 0 and 2π).

3. Figure of merit (FOM)

The genetic algorithm is only as powerful as its FOM. Based upon previous experience working with the phase restoration problem for 2-D surface structures [15–17], a useful FOM that was found is of the form

$$\mathrm{FOM} = \Sigma |J_{k-1}(\beta) - J_k(\beta)|^2 \tag{10}$$

where $J_{k-1}(\beta)$ are the moduli and phase of the $(k-1)$th iteration in the error-reduction algorithm and $J_k(\beta)$ are the moduli and phase for the kth iteration. Eq. (10) is similar to the FOM used by Fienup [8].

The former FOM is calculated in reciprocal space. However, it is also known that once the solution has been projected and inverse Fourier transformed into real space, the true solution should conform to zero outside the region of the object domain constraint. Hence, before any support constraints are applied, a second FOM is calculated (FOM_o) which is defined as

$$\mathrm{FOM}_o = 1 - \frac{\sum_{|x|<a/2} |j(x)|^2}{\sum_x |j(x)|^2} \tag{11}$$

where $j(x)$ is the inverse Fourier transform of the reciprocal space moduli and phases. The final FOM used by the genetic algorithm as an estimate of the goodness of fit is

$$\mathrm{FOM\_SUM} = \alpha\,\mathrm{FOM} + \beta\,\mathrm{FOM}_o \tag{12}$$

where α and β are constants to control the relative contributions of the real space and reciprocal space calculated FOMs.

4. Calibration of the FOM

Accuracy of the FOM was determined using a second 'correctness' factor (CFOM) which monitors

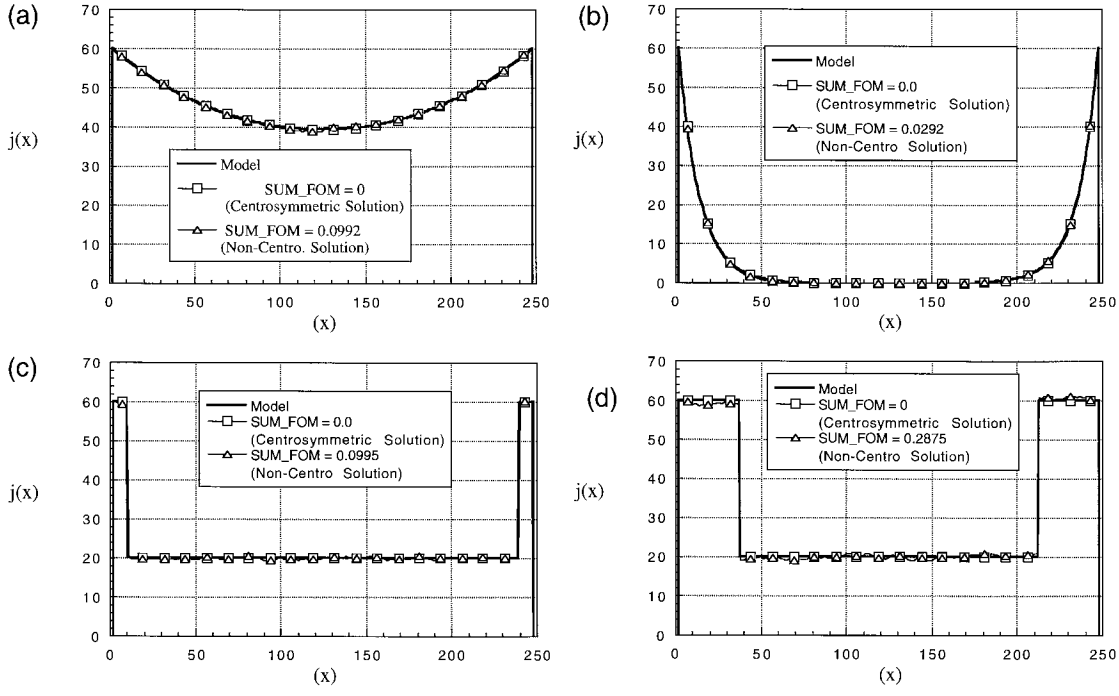

Fig. 4. Sinusoidal (a) and (b) and square (c) and (d) models. For all models the centrosymmetric solution corresponded to a zero FOM.

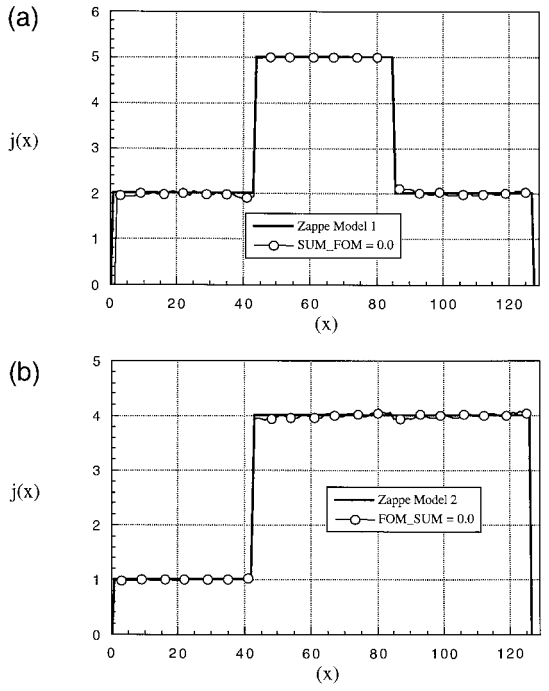

Fig. 5. Two different possible solutions from the same starting $I_c(\beta)$ data from Zappe. Model (a) is a centrosymmetric solution and (b) is a non-centrosymmetric solution. Both solutions correspond to a zero FOM.

the accuracy of the phases determined by the algorithm to the true phases for a given model. This CFOM is defined as

$$\mathrm{CFOM} = \frac{1}{N}\Sigma|1 - \cos(\phi_c(\beta) - \phi_t(\beta))| \qquad (13)$$

where $\phi_c(\beta)$ is the calculated phase, $\phi_t(\beta)$ the true phase, and N the number of phases used for the restoration. Fig. 3 is an example of the calculated FOM and corresponding CFOM for four different total numbers of iteration within the phase restoration algorithm. The CFOM vs. FOM plots were calculated for the asymmetric model described by Zappe [4].

It is important to note that any starting set of phases will converge towards a small FOM; however, correct solution sets seem to converge more quickly (more locally convergent). Thus, possible correct solutions can be distinguished from poor solutions based on the relative speed of convergence. Fig. 3 shows that for a fixed number of iterations the correct solution converges faster to a low FOM. Increasing the number of iterations improves the overall convergence (reduces the FOM) of each solu-

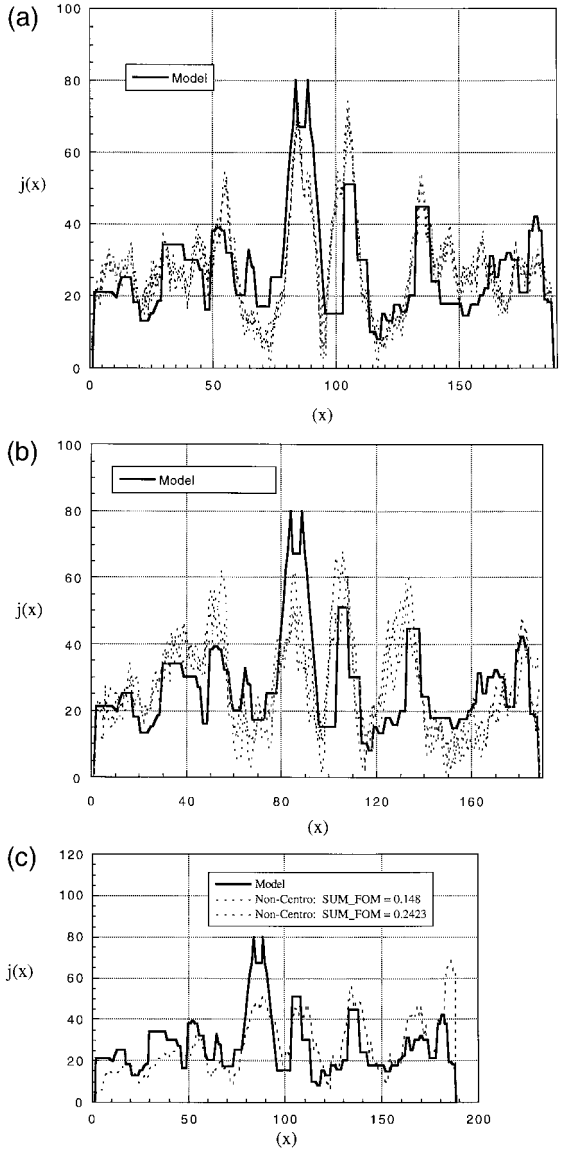

Fig. 6. Complex boundary model: (a) 100 iterations using the centrosymmetric constraints on the phase values such that all phases must be either 0 or 180°; (b) 1000 iterations using the same initial phases as in (a) but allowing the phase values to be any value between 0 and 360° for the last 900 iterations (pseudo-centrosymmetric); (c) non-centrosymmetric solution allowing starting phases to vary from 0–360°.

tion, however, the relative difference between solutions remains (see Fig. 3a–d). Thus, there is no added benefit to running each possible set of phases for a large number of iterations. After a final solution set is obtained, each solution may then be run for a larger number of iterations thus reducing the overall calculation time and improving the speed of the algorithm.

5. Test models

The phase retrieval algorithm described above in conjunction with the genetic algorithm was used to solve the phase problem for a number of test models, 256 pixels across.

Fig. 4a–d are square and sinusoidal models from Barone [18] used for testing the algorithm. In all of the above models from Barone, only one solution for each model was found and it corresponded to the known correct solution. Inspection of the graphs shows small oscillations about the true solution.

Fig. 5a–b are two different real space models from Zappe [4] that are known to have identical Fourier moduli $|J(\beta)|$ but different phases $\phi(\beta)$. By using the same Fourier moduli, the phase retrieval algorithm was able to find both solutions (sets of phases).

Fig. 6a–c is the model designed to represent a complicated boundary structure (it is in fact a profile of Chicago). A pseudo-centrosymmetric search approach described above was found to give the best fit to the model. Although the solution did not correspond to an exact fit, the algorithm was able to find solutions that had the correct 'feel' which will be discussed more detail below.

6. Discussion

The phase problem for 1-D objects is notoriously difficult to solve since the possibility exists for multiple solutions. Any real space object $j(x)$ that is consistent with all of the available constraints is a possible (feasible) solution. It is important to mention that without making assumptions about the object $j(x)$ it would be impossible to distinguish between two different solutions, both with a zero FOM. When evaluating the test models above, three different types of solutions were observed.

6.1. Type I

The first type of solution was one in which the real space object was found to have only one solution. Thus, any starting set of phases that were given to the phase-retrieval algorithm resulted in the same unique solution. The test models from Barone [18] are examples of this type. Type I solutions (Fig. 4) are ideal since they are unique and need no further interpretation. The solution is simply the restored current density profile $j(x)$.

6.2. Type II

The second type of solution was one in which there existed multiple real space objects that when Fourier transformed produce the same Fourier Moduli $I_c(\beta)$. The model from Zappe (Fig. 5) is an example of this type of solution. Type II solutions have previously been considered the stopping point for working with the 1-D phase restoration problems. Variations in the initial phases would result in different solutions and determining the 'correct' solution was considered impossible without making further assumptions about the real space object $j(x)$.

We have taken a different approach to the problem. Instead of attempting to make assumptions about $j(x)$, we simply use the real space constraints mentioned earlier to limit the number of possible solutions. By using the known constraints on $j(x)$, we are able to reduce the number of possible solutions which are consistent with the boundary conditions. We have solved numerous models from simple symmetric cases to complex random models, and without exception, the number of solutions that are found within the box has been limited to ≈ 2–3 different solutions per model. Finding a small set of solutions that contains the correct solution would be a vast improvement over the existing options. However, it is known that the current density is dependent on the microstructure of the boundary. Thus when multiple solutions to the 1-D phase problem exist (type II solutions), it is possible to compare the small number of possible current density maps calculated by the phase retrieval algorithm to the microstructure of the boundary and determine the one correct solution.

6.3. Type III

The third type of solution that was found was the least desirable of the three types. For type III solutions (Fig. 6), the phase retrieval algorithm was not able to correctly restore the phases such that a perfect match between the model and the restored solution was found. However, the algorithm was able to produce a profile $j(x)$ that exhibited the correct 'feel' to the solution. Peaks and valleys in the solution corresponded to peaks and valleys in the model and in most cases the relative height of the peaks was correct, but the absolute value of the solution was incorrect. Consequently, the restored model was only good for qualitative comparison. Fortunately, type III solutions are usually distinguishable from type I and type II solutions. For a type III solution, the top 10 or 20 solutions all had the same 'feel' (were qualitatively the same) but they were all slightly different. For a type II solution the top 20 FOMs all corresponded to a small set (2–3) of solutions while there was only one solution for a type I. Therefore, it is quite easy to distinguish type I and II solutions from type III solutions.

Unfortunately, the number of possible solutions is dependent on the shape of the real space object $j(x)$. Therefore, it is not possible to know a priori what type of solution one may be dealing with. Since there may always exist multiple solutions to the problem, it is not necessarily important to be able to find a unique solution using the phase retrieval algorithm, but rather it is more important to be able to find all possible solutions. The phase retrieval algorithm used for the test cases above has been extremely successful in finding all of the solutions for a given problem.

Since the shape of the object is unknown, it is important to know as accurately as possible the constraints that will be used to limit the number of solutions. Definition of the width of the junction (dimension a from Fig. 1) is important since the set of all possible solutions must fall within the width of the junction. If the width for the junction used in the phase restoration algorithm is too wide, solutions may exist in the final set that do not represent a possible current density profile. If the width used for the restoration is less than the actual width it may result in the elimination of possible solutions from the final solution set. Therefore, it is important to use the width corresponding to the actual measured width of the junction.

The critical current density J_c is used to place an upper limit on the possible solution profiles. J_c is a bulk property defined as the critical current I_c carried by the junction divided by the cross-sectional area of the junction. The width of the junction used to calculate the area and the actual width of the junction that is carrying supercurrent is not always the same. Variations of the microstructure along the length of the boundary may result in non-superconducting regions along the boundary. Thus, the actual width of the junction carrying supercurrent can be less than the measured width of the boundary. This may result in over estimation of the cross-sectional area of the boundary and consequently an underestimation of J_c. Unfortunately, different values of J_c used in the phase restoration algorithm can result in adding or subtracting solutions from the final solution set. We have taken care to overestimate the value of J_c so as not to eliminate possible correct solutions.

The specific parameters used to optimize the genetic algorithm search routine are strongly problem dependent. Although the parameters are problem dependent, the genetic algorithm has one major advantage over other minimization techniques. It searches solution space without any a priori information on the function that is being minimized. The experimentally measured moduli, the real space constraints on the junction and the initial parameters for the genetic algorithm are all that is needed to begin the search algorithm. It has also been shown to be more efficient than standard random number generators or grid searches for a similar class of problems, 2-D surface crystallographic phase restorations [15,16].

7. Conclusion

By using a phase retrieval algorithm similar to the Gerchberg–Saxton error-reduction algorithm with a generalized projection onto sets form, it is possible to restore the phase information that is not measured when experimentally recording $I_c(\beta)$ data for Josephson junctions without making any assumptions about the current density distribution $j(x)$. In general, it is not possible to find a unique solution

for the 1-D phase problem; however, it is possible with the assistance of the genetic algorithm to efficiently find all possible solutions. If multiple solutions exist for a junction, the set of all possible solutions can be compared against the boundary microstructure and the correct solution can be determined.

Acknowledgements

This work was supported by the National Science Foundation Office of Science and Technology Centers, under contract No. DMR 91-20000 (MC and LDM) and the United States Department of Energy, Basic Energy Sciences-Materials Science, under contract No. W-31-109-ENG-38 (KLM) and National Science Foundation grant No. DMR-9214505 (EL).

References

[1] B.D. Josephson, Adv. Phys. 14 (1965) 431.
[2] R.C. Dynes, T.A. Fulton, Phys. Rev. B 3 (1971) 3015.
[3] A. Papoulis, The Fourier Integral and Its Applications, McGraw-Hill, New York, 1962.
[4] H.H. Zappe, Phys. Rev. B 7 (1975) 2535.
[5] R.W. Gerchberg, W.O. Saxton, Optik 35 (1972) 237.
[6] R.W. Gerchberg, Opt. Acta 21 (1974) 709.
[7] J.R. Fienup, Opt. Lett. 3 (1978) 27.
[8] J.R. Fienup, Appl. Opt. 21 (1982) 2758.
[9] M.I. Sezan, Ultramicroscopy 40 (1992) 55.
[10] A. Levi, H. Stark, Image Recovery: Theory and Application, Restoration from Phase and Magnitude by Generalized Projections, Academic Press, 1987, pp. 277–320.
[11] P.L. Combettes, Adv. Imaging Electron Phys. 95 (1996) 155.
[12] J.H. Holland, Adaptation in Natural and Artificial Systems, University of Michigan Press, Ann Arbor, 1975.
[13] D.E. Goldberg, 1989, Genetic Algorithms in Search Optimization and Machine Learning, Addison-Wesley Publishing, New York, 1989.
[14] J.E. Baker, Proceedings of an International Conference on Genetic Algorithms and Their Applications, Erlbaum, Hillsdale, NJ, 1985.
[15] E. Landree, C. Collazo-Davila, L.D. Marks, Acta Cryst. B 53 (1997) 916–922.
[16] L.D. Marks, E. Landree, Acta Cryst. A 54 (1998) 296.
[17] J.C. Dainty, J.R. Fienup, Image Recovery: Theory and Application, Academic Press, 1987.
[18] A. Barone, Physics and Applications of the Josephson Effect, Wiley, 1982.